JOURNAL OF MATERIALS SCIENCE 31 (1996) 3003–3008

Gaseous corrosion mechanisms of silicon carbides in Na_2SO_4 and V_2O_5 environments

WEN C. SAY, SIANG C. LIU
Department of Materials and Mineral Resources Engineering, National Taipei Institute of Technology, Taipei, Taiwan, 10626

Hot-pressed polycrystalline SiC (HPSiC) and single crystal SiC (SCSiC) were exposed to Na_2SO_4 and V_2O_5 vapours at 1000 °C. Vapours were carried by the argon gas over the specimens where corrosion studies were conducted. Mixed-kinetics mechanisms for HPSiC under gaseous environments have been developed in the form of corrosion weight loss per unit area with time. The decomposed gases diffusing through the SiO_2 film and the reaction products at the substrate surfaces are the two major steps that contribute to the overall reaction for this material. SCSiC was observed to have severe corrosion attacks on its surfaces and corrosion pits with honeycomb shapes were left.

1. Introduction

Previous work [1] and many other investigators [2–7] have shown that the formation of a thin, passive oxidation scale (SiO_2) on the exposed surfaces of silicon carbide may provide the substrate with excellent corrosion resistance. However, under severe conditions, active dissolution of the SiO_2 scale will be attributed to the corrosion of SiC. Most accelerated corrosion of SiC has been reported in the presence of basic salts [5, 6], silicate melts [7, 8], coal slag [9, 10], and metallic oxides [1, 2, 11]. Nevertheless, SiC is still considered as one of the best candidate materials which can be applied in gaseous combustion environments such as gas turbine components, heat exchanger devices [12], and industrial furnaces [13, 14]. It is therefore important to understand how this material is affected by gaseous corrosions.

Early investigations of the corrosion of silicon carbide in gaseous atmospheres [15, 16] have shown that the materials is gasificated and corroded on exposure to low P_{O_2}. Afterwards, SiC in gas–salt corrosion environments has been concerned with the presence of various salts [2]. This study indicates that hot corrosion behaviour of SiC, critical when in contact with alkaline salts, depends critically on the effects of ambient partial pressure of oxygen. Furthermore, later investigations [1, 7, 8] have shown that SiC can also be severely corroded under non-basic salt environments. On the other hand, Federer and co-workers [13, 14, 17, 18] have done a series of works showing that SiC is corroded by alkali halides and sodium sulphate vapours in an oxidizing atmosphere. Sodium halides or sulphates were vapourized then transported by air and water vapour to the ceramics held at 1200 °C. Based on conditions favouring corrosion thermodynamics, corrosion mechanisms were studied. They concluded that corrosion may be regarded as the chemical alternation of the normally protective SiO_2 film by Na_2O. In spite of these studies dealing with corrosion behaviour of SiC, detailed kinetic descriptions of the nature of corrosion attacks on SiC are not mentioned in the literature.

The purpose of this paper is to link thermochemical activities of SiC with the reaction kinetic derivation in a system of gaseous corrosion. Vapourized media, Na_2SO_4 and V_2O_5 vapours, were chosen as the corroding environments. Sodium sulphate has been reported many times [2, 4, 5, 6, 18] as being a critical substance in corrosion reaction with the protective SiO_2 layer. Molten V_2O_5 was proven to cause severe corrosion on SiC in a previous work [1]. Corrosion by V_2O_5 vapour is verified here for further comparison. This study also examines results of gaseous corrosion on different types of SiC. It is shown that silicon carbides in polycrystalline alpha-phase and single crystal form exhibited different corrosion behaviours.

2. Experiments

2.1. Materials

Both polycrystalline hot-pressed alpha-SiC (HPSiC) and single crystal SiC(SCSiC) obtained from Hitachi, Japan were used in this study. HPSiC was hot-pressed and sintered from SiC powders with three different particle sizes which were mixed. The additives and major impurities of this material are listed in Table I [19]. The as-received SCSiC having a growth direction in (0001) was observed using electron microscopy. HPSiC specimens were cut into 1 mm × 25 mm × 25 mm blocks. SCSiC specimens were measured and sieved to have weights of 22 ± 2 mg. All the samples were ground to provide fresh surfaces before each test. Reagent grade Na_2SO_4 and V_2O_5 were used as the vapourized media for the gaseous corrosion tests.

TABLE I Composition for HPSiC powders

No.	Average particle size (μm)	Additives and impurities (%)									
		Free SiO_2	Free Si	Free C	Al	Ti	V	Cr	Fe	Ni	Cu
1	0.5	2.33	1.99	0.90	0.016	0.14	0.047	0.007	0.014	0.028	0.001
2	0.7	2.72	1.72	0.50	0.16	0.16	0.058	0.007	0.013	0.020	0.001
3	2.0	2.18	0.86	0.31	0.008	0.16	0.043	0.007	0.009	0.023	0.001

2.2. Apparatus

A Nobeltherm Model RHT0817 programmable tube furnace was used for the corrosion tests. Samples were exposed to the gaseous environments in the apparatus shown in Fig. 1. Argon (99.9% purity) acting as the carrier gas, was passed through a purifier and dryer. This highly purified gas was metered by needle valves at a flow rate of 6.67 cc per minute before being introduced into the tube furnace.

2.3. Procedures

Inside the tube, sodium sulphate or vanadium oxide powders were placed in an alumina boat and heated ($\sim 7\,^{\circ}\mathrm{C\,min^{-1}}$) above their melting points and held at 1000 °C for vapourization. The carrier gas flowed through the vapourized media and over the specimens where corrosion behaviours were produced. Diluted HF solution and hot deionized water treatments were used after each test, refer to previous work [1]. Weight loss measurements were combined with atomic absorption spectroscopy and electron microscopy to characterize this study.

3. Results and discussion

3.1. Corrosion of HPSiC in Na_2SO_4 gaseous environments

Some researchers have suggested that sodium sulphate will not react with the SiO_2 protective layer on

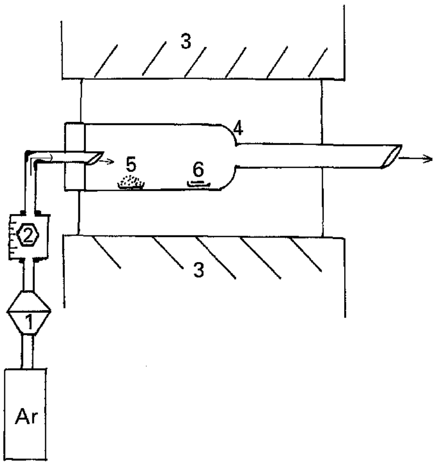

Figure 1 The apparatus for performing gaseous corrosion tests. Key: 1 gas purifier and dryer; 2 gas valve and flow fire adjustment; 3 high temperature tube furnace; 4 zirconia tube; 5 Na_2SO_4/V_2O_5; 6 silicon carbide specimen.

SiC substrate unless it is in the presence of excess carbon or small amounts of basic oxides [4–6]. This is simply based on the consideration of favourable thermodynamic mechanisms. In the study of gaseous corrosion, the key issue should focus on the relationship between SiC substrates and decomposed Na_2SO_4 products at equilibrium state. The thermal constants of sodium sulphate and its decomposition are referred to in Table II [20]. The following dissolving equilibrium equations and their Gibbs' free energies are then suggested at 1000 °C (Na_2SO_4 is decomposed above its melting point, 884 °C):

$$Na_2SO_{4(l)} = Na_2S_{(s)} + 2O_{2(g)}$$

$$G_r = 585.70\ \mathrm{kJ\,mol^{-1}} \qquad (1)$$

$$Na_2SO_{4(l)} = Na_2S_{(s)} + SO_{2(g)} + 1/2O_{2(g)}$$

$$G_r = 356.30\ \mathrm{kJ\,mol^{-1}} \qquad (2)$$

$$Na_2S_{(s)} + 3/2O_{2(g)} = Na_2O_{(s)} + SO_{2(g)}$$

$$G_r = 229.3\ \mathrm{kJ\,mol^{-1}} \qquad (3)$$

$$Na_2S_{(s)} + O_{2(g)} = 2Na_{(g)} + SO_{2(g)}$$

$$G_r = 13.30\ \mathrm{kJ\,mol^{-1}} \qquad (4)$$

$$Na_2O_{(s)} = 2Na_{(g)} + 1/2O_{2(g)}$$

$$G_r = 215.60\ \mathrm{kJ\,mol^{-1}} \qquad (5)$$

The free energy of the reaction in the equilibrium state can be described by the Nernst equation:

$$G_r = -RT\ln K \qquad (6)$$

where K is the equilibrium constant. The subscript "r" stands for the reactive species. If the activities of decomposed products in the solid state are unity, by applying Equation 6, the partial pressures of oxygen (P_{O_2}), sulphur dioxide (P_{SO_2}), and the sodium gases (P_{Na}) in equations 1 to 5 will be 1.76×10^{-7}, 3.77×10^{-4}, and 4.03×10^{3} Pa, respectively. When corrosion of SiC occurs in the above gaseous environments the following familiar reaction will occur first with favourable free energy:

$$SiC + 3/2O_{2(g)} = SiO_2 + CO_{(g)}$$

$$G_r = -842.9\ \mathrm{kJ\,mol^{-1}} \qquad (7)$$

When P_{O_2} in Equation 7 remains at its equilibrated value the partial pressure of carbon monoxide (P_{CO}) reaches up to 1.60×10^{21} Pa. Hence it can be expected that CO gas, with this high escaping pressure, must erupt outwardly through the SiO_2 glassy film and

TABLE II Temperature constants of sodium sulphate and its decomposition products

Name	Synonyms and formula	Melting point (°C)	Boiling point (°C)
Sodium sulphate	Na_2SO_4	884	dissolved
Sodium oxide	Na_2O	sublimated 1275	–
Sodium sulphide	Na_2S	1180	–
Sodium	Na	98	883

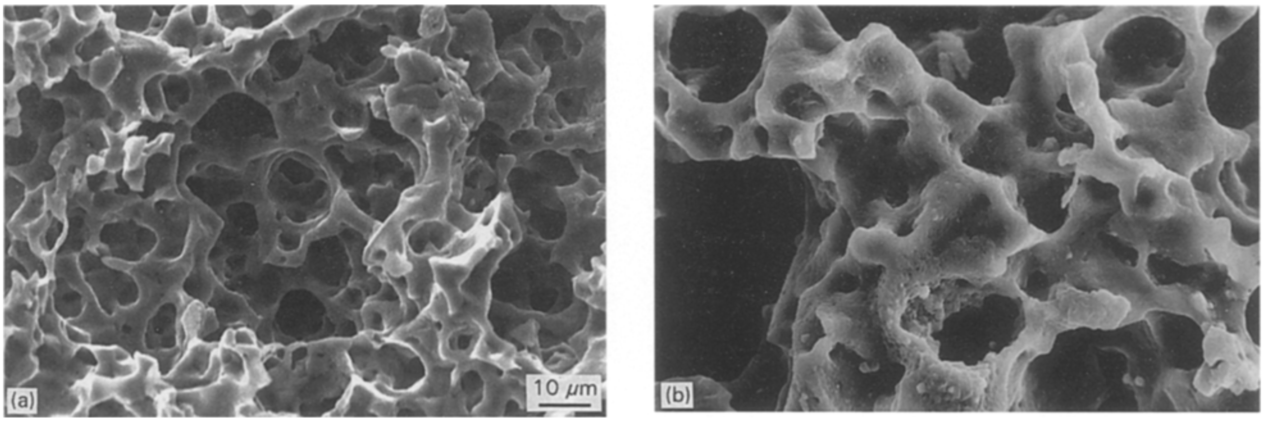

Figure 2 HPSiC morphologies after gaseous corrosion in Na_2SO_4 environments for 150 h at 1000 °C (a) 660 × (b) 990 ×.

penetrate inwardly into the SiO_2/SiC interfaces. Rapid evolution of CO gas will enhance SiO_2 dissolution which causes Equation 7 to move continuously to the right. Fig. 2 shows tunnel-like channel microstructures of HPSiC after Na_2SO_4 gaseous corrosion for 150 h at 1000 °C. The morphologies of the retained concavities on the substrate surfaces provide evidence of the tremendous force of the evolved gas. Furthermore, with the agitation due to CO eruption, SiO_2 would actively react with Na_2O resulting in the formation of sodium silicates [21] and this leads to the final state of the SiC consumption. Fig. 3 presents the rate of SiC hot corrosion under Na_2SO_4 vapour at 1000 °C. It can be noted from this figure that the rate of weight loss increases with corrosion time initially and then slows down after 8 days of sweeping. This suggests that the corrosion reaction may occur as a series of rate controlling steps.

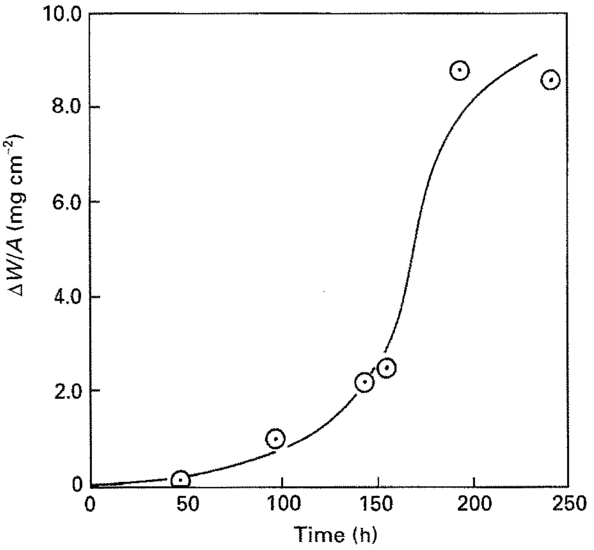

Figure 3 Weight loss per unit area of HPSiC in Na_2SO_4 gaseous environments as a function of time at 1000 °C.

The Na_2SO_4 decomposition gases diffuse through the SiO_2 protective film and the decomposition reactions on the surfaces of the SiC are assumed to be the two major steps that contribute to the overall corrosion mechanisms in gaseous environments. If K_s represents the surface reaction rate constant and P_g^s is the pressure of Na_2SO_4 decomposition gases at the SiO_2/SiC interface, the rate of reaction, weight loss per initial area and time ($\mathrm{d}W/A/\mathrm{d}t$), may be expressed by:

$$\frac{\mathrm{d}W/A}{\mathrm{d}t} = K_s P_g^s \tag{8}$$

The rate is also known from the diffusion rate of the corrosive gases through the solid–liquid (SiC/SiO_2) boundary layer, δ. In this case, the rate can be represented by applying Fick's first law with an appropriate stoichiometry factor, σ:

$$\frac{\mathrm{d}W/A}{\mathrm{d}t} = D_g \frac{P_g^o - P_g^s}{\sigma\,\delta} \tag{9}$$

where D_g and P_g^o stand for the diffusivity and the pressure of ambient decomposed gases, respectively. The positive signs in Equations 8 and 9 indicate that the reaction is toward the SiC substrate surfaces. This P_g^s may be solved, under steady state for P_g^s giving

$$P_g^s = P_g^o - \frac{\sigma\,\delta}{D_g}\frac{\mathrm{d}W/A}{\mathrm{d}t} \tag{10}$$

Equating Equations 10 and 8 and rearranging gives the result:

$$\frac{\mathrm{d}W/A}{\mathrm{d}t} = \frac{P_\mathrm{g}^\circ}{\dfrac{1}{K_\mathrm{s}} - \dfrac{\sigma\,\delta}{D_\mathrm{g}}} \tag{11}$$

The reaction is the formation of the SiO_2 layer on the solid SiC surface through which the steady-state corroding diffusion occurs. The product of σ and δ is reasonably transformed into the difference between the initial weight (W_o) and the remaining weight (W_r) per unit area with a proportional factor β

$$\sigma\,\delta = \beta\left(\frac{W_\mathrm{i}}{A} - \frac{W_\mathrm{r}}{A}\right) = \beta\,\frac{\Delta W}{A} \tag{12}$$

The value $\Delta W/A$ represents the weight loss per unit area at any time. Equation 11 can be integrated for constant pressure of ambient corrosion gases and given as an expression for time, t:

$$t = \frac{(\Delta W/A)}{K_\mathrm{s}\,P_\mathrm{g}^\circ} - \frac{\beta\;(\Delta W/A)^2}{D_\mathrm{g}} \tag{13}$$

By rewriting Equation 13

$$\frac{t}{\Delta W/A} = (K_\mathrm{s} P_\mathrm{g}^\circ)^{-1} \beta D_\mathrm{g}^{-1}\left(\frac{\Delta W}{A}\right) \tag{14}$$

A plot of the left hand side of Equation 14 ($t/\Delta W/A$) against $\Delta W/A$ results in a straight line having a negative slope and positive intercept values. The diffusion term in Equation 14 can be represented by the slope of the straight line which is the negative product of the proportional factor and reciprocal of the corrosion gases diffusivity ($-\beta \times D_\mathrm{g}^{-1}$). The intercept represents the surface reaction term containing the reciprocal product of the rate constant and ambient gas pressure $(K_\mathrm{s} \times P_\mathrm{g})^{-1}$. Fig. 4 illustrates this linear relationship by applying the data in Fig. 3. Consistency of the plot with the predicted equations indicated that the above derivation is applicable to the corrosion mechanisms for HPSiC specimens. The values of the slope, -7.2, and intercept, $+85.0$, obtaining from this figure, confirm the proposed kinetics. The system can certainly be described as a mixed surface reaction with gas transport through the SiO_2 protective diffusion layer contributing to the overall mechanism.

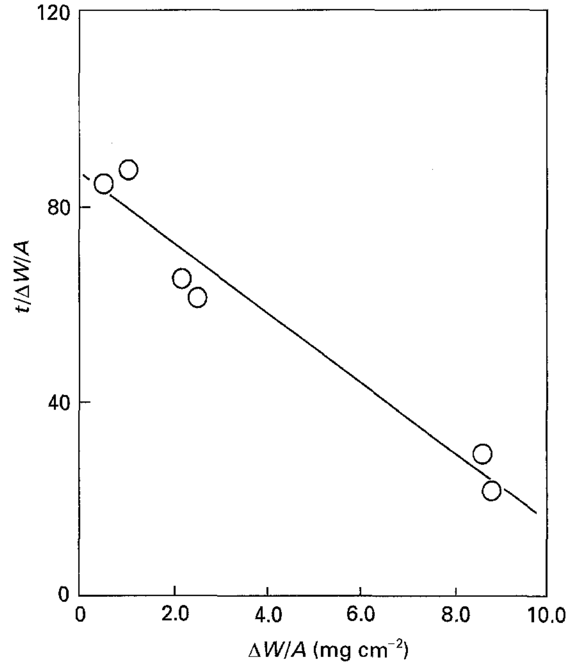

Figure 4 Plot of $t/\Delta W/A$ versus $\Delta W/A$ for mixed kinetics of HPSiC in Na_2SO_4 gaseous environments at 1000°C (○ measured; — calculated).

3.2. Corrosion of SCSiC in Na_2SO_4 gaseous environments

The SCSiC morphologies after 155 h of Na_2SO_4 gaseous corrosion at 1000 °C are shown in Figs 5 and 6. Numerous corrosion pits with honeycomb shapes on each stacking layer are randomly distributed at different sizes and depths (Fig. 5). This may be described that the decomposed gases shovel up the SCSiC hexagonal structures by diffusing through solid surfaces and to the opposite c-axis direction of the lattices (Fig. 6). However, the complicated geometry and the irregular open porosities resulting from the gaseous corrosion have made rate studies of SCSiC (weight loss per unit area with time) impossible. Fig. 7 shows

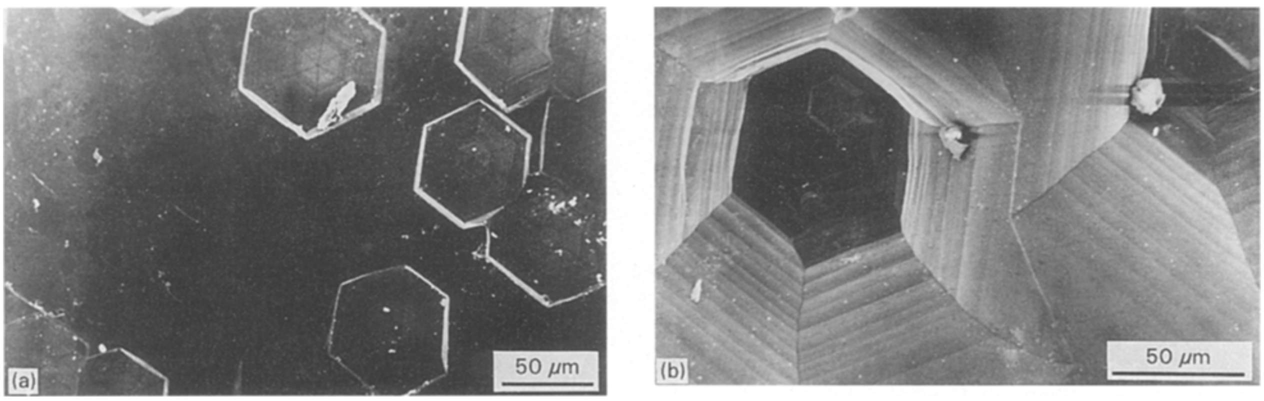

Figure 5 Randomly distributed corrosion pits of different size (a) and at different depths (b) on SCSiC after exposure to gaseous Na_2SO_4 environments for 155 h at 1000 °C

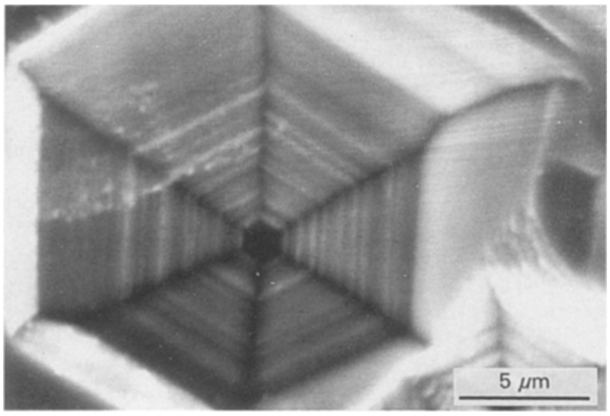

Figure 6 Na_2SO_4 decomposition gases penetrate through to the opposite *c*-axis direction in the SCSiC hexagonal structure.

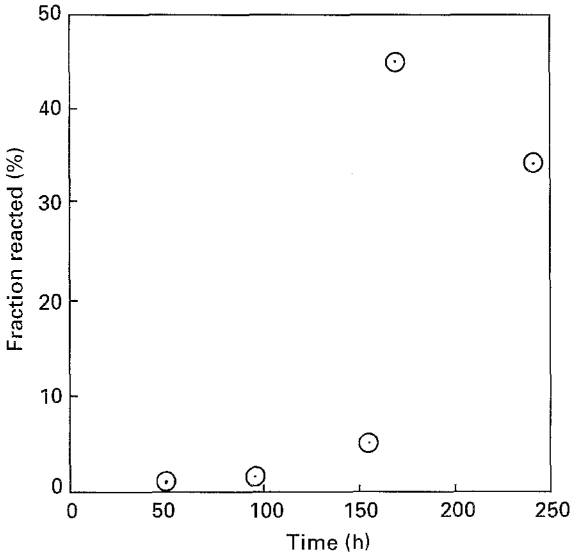

Figure 7 Results of the fraction SCSiC reacted in gaseous Na_2SO_4 environments at 1000 °C

that the fraction of SCSiC reacted as a result of corrosion is scattered for different time intervals.

3.3. Corrosion of HPSiC in V_2O_5 gaseous environments

HPSiC in the gaseous V_2O_5 environment is studied next. Vanadium oxide decomposed into its suboxidizing states at 1000 °C (the melting point of V_2O_5 is 690 °C):

$$V_2O_{5\,(l)} = V_2O_{4(s)} + 1/2O_{2(g)}$$
$$G_r = 1027.79 \text{ kJ mol}^{-1} \qquad (15)$$

$$V_2O_{4\,(s)} = V_2O_{3(s)} + 1/2O_{2(g)}$$
$$G_r = 966.86 \text{ kJ mol}^{-1} \qquad (16)$$

$$V_2O_{3\,(s)} = 2V_2O_{(s)} + O_{2(g)}$$
$$G_r = 890.56 \text{ kJ mol}^{-1} \qquad (17)$$

$$VO_{(s)} = V_{(s)} + 1/2O_{2(g)}$$
$$G_r = 320.03 \text{ kJ mol}^{-1} \qquad (18)$$

The partial pressures of oxygen dissociated from the above reactions will be 1.28, 7.49×10^{-2}, 7.51×10^{-16}, and 1.93×10^{-21} Pa, respectively. By using Equation 6 again and substituting each P_{O_2} value into Equation 7, P_{CO} will be 3.99×10^{31}, 5.60×10^{29}, 5.64×10^{8}, and 2.34 Pa, respectively. The high evolution pressures of the carbon monoxide gas enhanced an active dissolution of the SiO_2 protective film and led to the corrosion of the SiC substrates. These conditions are similar to those described in Section 3.1. However, it should be noted, P_{CO} and P_{O_2} equilibrated at in Reaction 18 and this is too low to oxidize SiC into SiO_2. (The VO is not able to reduce to the metallic vanadium form.) Fig. 8 reveals similar rough and con-

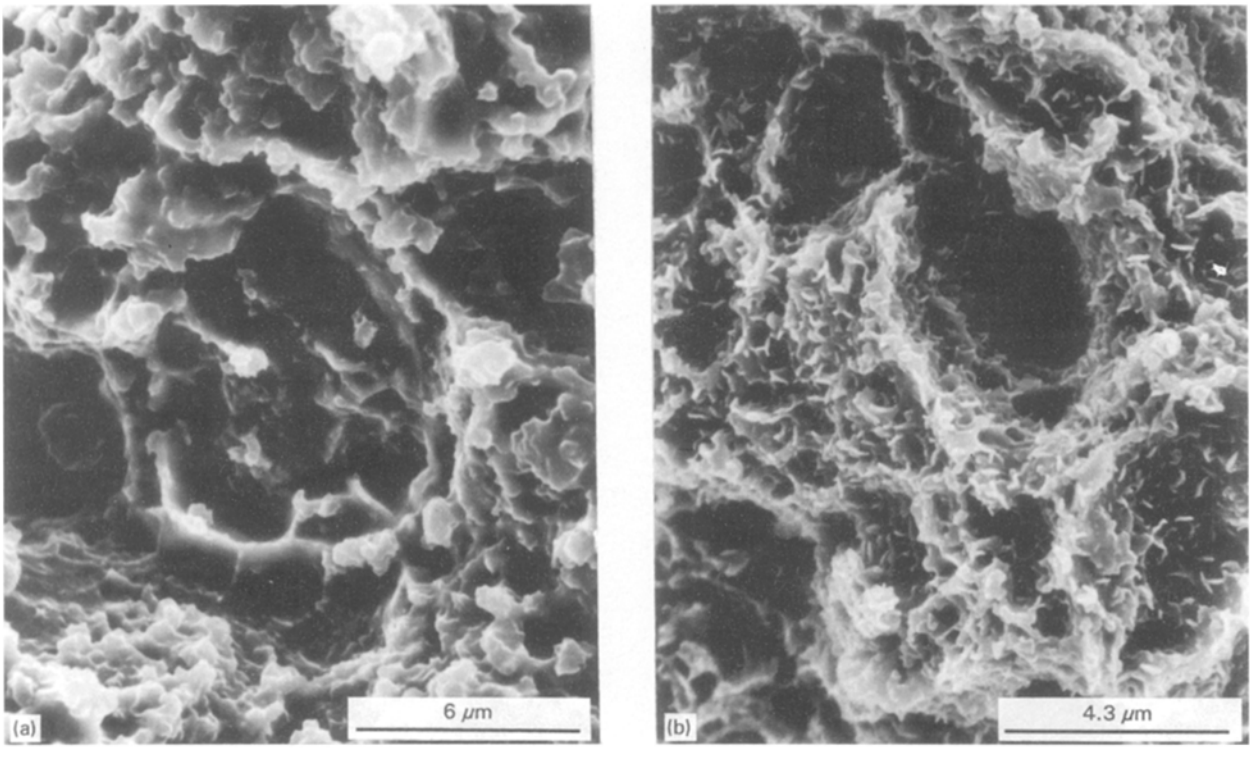

Figure 8 HPSiC morphologies after exposure to V_2O_5 gaseous environments for 200 h at 1000 °C (a) 3750 (b) 5250.

cave corrosion surfaces on HPSiC after exposure to the gaseous V_2O_5 and its suboxides, V_2O_4, and V_2O_3.

4. Conclusions

The results of a laboratory investigation of gaseous corrosion of silicon carbides have been presented. The findings of this research are concluded below:

1. Silicon carbides were corroded by the gaseous decomposition products of Na_2SO_4 and V_2O_5 at a temperature of 1000 °C.
2. Starting materials, HPSiC (hot-pressed SiC) and SCSiC (single crystal SiC), exhibited different influences on their corrosion mechanisms. Linear kinetics for HPSiC gaseous corrosion were obtained. Corrosion kinetics of SCSiC were difficult to determine due to the variation of its surface properties.
3. Mixed kinetics were suggested for HPSiC by Na_2SO_4 gaseous corrosion. The decomposition gases of Na_2SO_4 diffused through the SiO_2 protective layer plus the products reacting at the surface were assumed to be two important steps which contributed to the overall reaction.
4. SCSiC was observed to have complicated geometries and severe etching on its surfaces after Na_2SO_4 gaseous corrosion.
5. Corrosion damage in HPSiC caused by gaseous V_2O_5 were also observed.
6. The refractory nature of the SiO_2 layer on the surfaces of different types of SiC was found to be permeable to the corrosion gases. Hence, surface pretreatments of SiC should be performed for applications where vapourized media may be contained or produced.

Acknowledgements

The authors wish to express their gratitude to ROC National Science Council for its support over three consecutive years, Grant No. NSC 80-0405-E027-03, NSC 81-0405-E-027-03, and part of NSC 82-0404-E-027-022.

References

1. W. C. SAY, J. K. WU and W. L. CHEN, *J. Mater. Sci.* **25** (1990) 1614.
2. D. W. McKEE and D. CHATERJI, *J. Amer. Ceram. Soc.* **59** (1979) 441.
3. J. R. BLACHERE and F. S. PETTIT, *DOE/ER*, Feb. (1984) 10915.
4. N. S. JACOBSON and J. L. SMIALEK, *J. Amer. Ceram. Soc.* **68** (1985) 432.
5. J. L. SMIALEK and N. S. JACOBSON, *ibid.* **69** (1986) 741.
6. N. S. JACOBSON, *ibid.* **69** (1986) 74.
7. D. P. BUTT and J. J. MECHOLSKY, *J. Amer. Ceram. Soc.* **72** (1989) 1628.
8. G. DRAZIC, R. FORTHMANN and A. NAOUMIDIS, *J. Mater. Sci.* **28** (1993) 2377.
9. P. F. BECHER, *J. Mater. Sci.* **19** (1984) 2805.
10. M. K. FERBER, J. OGLE, V. J. TENNERY and T. HENSON, *J. Amer. Ceram. Soc.* **68** (1985) 191.
11. G. ERVIN, Jr., *ibid.* **41** (1985) 347.
12. B. E. DAWSON (ed.), "Physical Science, Heat Engines" (Nuffield Foundation by Penguin Books) (Heineman Education, Sandford, USA) p. 514.
13. J. I. FEDERER, T. N. TIEGS, D. M. KOTCHICK and D. PETRAK, Oak Ridge National Laboratory **TM-9677** (1985) (Oak Ridge, Tennessee).
14. J. I. FEDERER and P. J. JONES, *ibid.* **9741** (1985).
15. J. E. ANTILL and J. B. WARBURTON, *AGARD Conf. Proc.* **52** (1970) 10 (NTIS AD-70257).
16. E. A. GULBRANSEN and S. A. JANSSON, *Oxid. Met.* **4** (1972) 181.
17. J. I. FEDERER, J. W. ROBBINS, P. J. JONES, and C. HAMBY, Jr., *ORNL/TM* **6258** (1985) Oak Ridge National Laboratory, Oak Ridge, Tennessee.
18. J. I. FEDERER, *Adv. Ceram. Mater.* **3** (1988) 56.
19. Y. TAKEDA, T. KOSUGI, S. IIJIMA and K. NAKUMURA, in Proceedings of the International Symposium on Ceramic Component for Engine, Japan, 1983 p. 529. Hitachi Research Laboratory, Japan.
20. R. C. WEAST (ed.) and M. J. ASTLE (Assoc. ed.), in "CRC Handbook of Chemistry and Physics", 62nd, Edn (CRC Press, Boca Raton, 1981–1982) p. B-150.
21. W. D. KINGERY, H. K. BOWEN and D. R. UHLMANN, in "Introduction To Ceramics" (Wiley, New York, 1976) p. 359.

Received 26 July 1994
and accepted 9 November 1995